Stabilizing and Improving Federated Learning with Non-IID Data and Client Dropout in IoT Systems

Jian Xu, Meilin Yang, Wenbo Ding, Member, IEEE, and Shao-Lun Huang, Member, IEEE

Abstract-Federated learning is an emerging technique for training deep models over decentralized clients without exposing private data, which however suffers from label distribution skew and usually results in slow convergence and degraded model performance. This challenge could be more serious when the participating clients are in unstable circumstances and dropout frequently. Previous work and our empirical observations demonstrate that the classifier head for classification task is more sensitive to label skew and the unstable performance of FedAvg mainly lies in the imbalanced training samples across different classes. The biased classifier head will also impact the learning of feature representations. Therefore, maintaining a balanced classifier head is of significant importance for building a better global model. To tackle this issue, we propose a simple yet effective framework by introducing a prior-calibrated softmax function for computing the cross-entropy loss and a prototype-based feature augmentation scheme to re-balance the local training, which are lightweight for edge devices and can facilitate the global model aggregation. With extensive experiments performed on Fashion-MNIST and CIFAR-10 datasets, we demonstrate the improved model performance of our method over existing baselines in the presence of non-IID data and client dropout.

Index Terms—Federated Learning, Data Heterogeneity, Client Dropout, Balanced-Softmax

I. INTRODUCTION

With the rapid development of Internet of Things (IoT) and machine learning techniques, significant amounts of data are generated in every day and can benefit intelligent applications in a wide variety of scenarios, such as speech recognition, healthcare systems and smart cities [1]-[3]. However, collecting data from edge devices for centralized model training causes high communication cost and serious privacy concerns, i.e., some data may contain personal and sensitive information [4]. As a result, training deep learning models centrally by gathering data from user devices might be impractical. To alleviate the above issues, it is attractive to adopt federated learning (FL) [5]-[7] to collectively train models, which can take full advantages of the local data and edge computational resources in the IoT systems. FL is a distributed computing paradigm where multiple edge devices, i.e., clients, collaboratively train a global model without disclosing local sensitive data. It usually consists of a central server and multiple clients,

Manuscript received. The research of Shao-Lun Huang is supported in part by the Shenzhen Science and Technology Program under Grant KQTD20170810150821146, National Key R&D Program of China under Grant 2021YFA0715202. (Corresponding author: Shao-Lun Huang.)

where each client updates the model based on local data and the server is responsible for synchronizing model parameters. The primary goal of FL is to efficiently train a global model with the highest possible accuracy [8], [9].

Despite the merits, FL in IoT systems is also confronted with various challenges, including high communication costs, security and privacy issues, system and data heterogeneity [10]. Data heterogeneity is also known as statistical heterogeneity or non-IID data, which means data across clients are drawn from different distributions and can have imbalanced quantities [11]. System heterogeneity could be caused by different resource constraints, including storage, computing capability, energy and network bandwidth [12]. In synchronous FL, aggregation is conducted when all the selected clients fully complete their local training and return their model updates. However, the clients could have significantly different performances in real-world scenarios, which implies that some faster clients have to wait for the slower ones, i.e., stragglers, resulting in unnecessary time-consuming. Moreover, some clients might be unresponsive due to inactive devices and/or communication failures and thus induce unavailability of some local updates, i.e., dropout. In this work, we focus on cross-device federated learning, where the participants are mostly edge devices such as smart phones and IoTs. These devices generally have limited computing and communication resources, and also have different training data distributions. Considering that federated learning typically takes a relatively large number of communication rounds to converge, it is difficult to ensure that all devices will be available or return back their local updates on time during the entire training process, leading to severe straggler and dropout issues [10].

To alleviate the straggler issue, FL algorithms usually perform partial participation and intermittent model aggregation after multiple local epochs as proposed in [5]. In such settings, however, the non-IID data brings new challenges for model aggregation due to the high diversity of local models. As a result, the resulting global model could have poor and unstable performance during the training process [11]. Moreover, it also takes more communication rounds for convergence and thus prolongs the on-clock training time. Therefore, developing FL algorithms with resilience to non-IID data and client dropout is of significant importance for fully taking advantages of scattered data generated from edge devices. Although tremendous efforts have been devoted to combating the non-IID data [13]— [15], the performance is still far from being satisfactory. While many factors can lead to the data heterogeneity among clients, the label skew is demonstrated to be the main reason of model performance deterioration as it could lead to inconsistency between local objectives and global objective [16]. On the other hand, previous works on centralized learning with long-tailed data and FL with class imbalance have demonstrated that the final decision layer is most vulnerable to class imbalance and will result in significant bias of decision boundaries [17]. To alleviate it, several methods including weight normalization of output layer and embedding augmentation of tail classes are investigated to rectify the model training for fair performance among all classes [17]. Inspired by those observations, we aim to train balanced classifiers during the local training stage to facilitate the global aggregation.

In this paper, we focus on mitigating the label skew and client dropout issues simultaneously, with especial interest in the case that each client only contains samples from a few categories. We emphases that the partial participation of clients is not a decision by algorithms and is uncontrollable due to unexpected client dropout. We propose a novel FL framework with Re-Balanced local classifier training (ReBaFL) that not only learns from the local data but also preserves the global knowledge. Specifically, we propose a relaxed version of priorcalibrated softmax function and a prototype-based feature augmentation scheme in local training to reduce the bias of local models, thus benefiting the aggregated global model. The proposed framework is evaluated on benchmark datasets with extensive experiments, which verify its effectiveness in stabilizing federated training while achieving a higher model accuracy, despite highly skewed label distributions across clients and severe client dropout. Our evaluation results show that non-trivial improvements in test accuracy can be obtained with slight extra communication overhead. To summarize, this paper makes the following contributions:

- A new FL framework with label prior calibrated local training scheme is proposed for alleviating catastrophic forgetting when local clients only observe partial labels.
- A prototype-based feature augmentation scheme is employed to further speed up the model convergence. Feature inverse attacks are also evaluated to indicate that using feature prototypes will not violate data privacy.
- The effectiveness of proposed framework is verified on Fashion-MNIST and CIFAR-10 datasets with various scenarios, where our method outperforms other baselines.

The rest of the paper is organized as follows. Section II reviews the related works. The background and motivation are introduced in Section III. The design of our framework is elaborated and evaluated in Section IV and Section V, respectively. Finally, Section VI concludes this paper.

II. RELATED WORK

A. Federated Learning with Non-IID Data

To address the non-IID data challenges in FL, a variety of works improve local learning algorithms by leveraging well-designed local regularization [8], [14], [15] and gradient bias correction [13], [18]. For example, FedProx [8] adds a proximal term to keep the updated parameter close to the original downloaded model, Scaffold [13] introduces control variates to correct the drift in local updates, and MOON

[15] adopts the contrastive loss to improve the representation learning. Class-balanced data re-sampling and loss reweighting methods could also be applied in FL to improve the model performance [19], [20]. However, this kind of approach cannot address the pathological case where data samples of some classes are missing on local clients. Moreover, data sharing mechanisms and data augmentation methods are also investigated to mitigate the non-IID data challenges [11], [21]. From the model aggregation perspective, selecting clients with more contribution to global model performance can also speed up the convergence and mitigate the non-IID issue [22]-[25]. However, the server needs to evaluate the clients in each round to decide the selection strategy, which introduces additional computational overhead to the system. In particular, it is possible to employ knowledge distillation techniques to obtain a global model, despite of the data heterogeneity across clients [26], [27]. Another line of work attempts to overcome data heterogeneity by developing personalized FL [28]-[31] or clustered FL [32]-[34]. Different from the above methods that only focus on non-IID data, this paper aims to improve the robustness in the presence of both data heterogeneity and device unavailability.

B. Tackling System Heterogeneity in FL

Another performance bottleneck faced by FL is the heterogeneous computing capacity and network bandwidth of clients. The straggler issue is caused by the delayed or lost uploading by some clients due to such system heterogeneity. Existing solutions choose to perform partial client participation [5] or allow clients to upload their local models asynchronously to the server [35]–[38]. A straggler-resilient FL is proposed in [39] that incorporates statistical characteristics of the local training data to actively select clients. An adaptive client sampling scheme is proposed in [40] to simultaneously tackle the system and statistical heterogeneity. Another line of work aims at dynamically adjusting the local workload according to the device capabilities by changing local batch size and local epochs [41], [42]. Client dropout is a more serious problem than stragglers since dropped clients simply have nothing to upload in the current round and can remain unavailable for a relatively long period. Hence, existing solutions for stragglers do not work well for this special issue. Some studies propose re-weighting aggregation rules or variance reduction methods to compensate the missing updates [43], [44].

III. PRELIMINARY AND MOTIVATION

A. Problem Formulation for Federated Learning

A typical implementation of FL system includes a cloud server that maintains a global model and multiple participating clients that communicate with the server through a network. We consider a setup with m clients that collaboratively train a global model under the coordination of cloud server without sharing raw private data. Mathematically, the underlying optimization problem can be formalized as follows:

$$\min_{\boldsymbol{w}} L(\boldsymbol{w}) = \sum_{i=1}^{m} \frac{|\mathcal{D}_{i}|}{|\mathcal{D}|} \underbrace{\mathbb{E}_{\xi_{i} \sim \mathcal{D}_{i}} \left[L_{i}(\boldsymbol{w}; \xi_{i}) \right]}_{:=L_{i}(\boldsymbol{w})}, \tag{1}$$

where \mathcal{D}_i denotes the local training data set drawn according to an underlying distribution $\mathcal{P}_i(X,Y)$ on $\mathcal{X} \times \mathcal{Y}$, where \mathcal{X} is the input space and $\mathcal{Y} = \{1,..,C\}$ is the label space. And we assume that generally $\mathcal{P}_i \neq \mathcal{P}_j$ for different client i and j, which is usually the case in FL. $L_i(\boldsymbol{w}_i;\xi_i)$ denotes the local loss function given model parameter \boldsymbol{w} and data point $\xi_i = (x_i,y_i)$ sampled from \mathcal{D}_i , which could be a general objective function, e.g., cross-entropy loss for classification tasks. We also denote \mathcal{D} the whole training data in the FL system. The global objective $F(\boldsymbol{w})$ can be regarded as a weighted average of local objectives and FL tries to minimize it in a distributed manner. For multi-class classification tasks, the local empirical risk is usually the cross-entropy between softmax outputs and ground-truth labels as in Eq. (2)

$$L_i = -\frac{1}{n_i} \sum_{j=1}^{n_i} \sum_{c=1}^{C} \mathbb{I}\{y_j = k\} \cdot \log\left(\frac{e^{z_j[c]}}{\sum_{c'=1}^{C} e^{z_j[c']}}\right), \quad (2)$$

where $\mathbb{I}(\cdot)$ is the indication function and z_j is the output logit. The most popular learning method FedAvg [5] works as follows. At each communication round t, the server selects a random subset S_t of clients to participate in this round of training. The server broadcasts the latest global model $\boldsymbol{w}^{(t)}$ to these clients for further local optimization. Then each participating client optimizes the local objective function based on the private data by its local solvers (e.g. SGD) with several local epochs E in parallel. Then, the locally-computed parameter updates $\Delta \boldsymbol{w}_i^{(t)}$ are collected and aggregated. Finally, the server updates the global model to $\boldsymbol{w}^{(t+1)}$ as in eq. (3) and finish the current round. In general, the FL task requires hundreds of rounds to reach the target accuracy.

$$\mathbf{w}^{(t+1)} = \mathbf{w}^{(t)} + \sum_{i \in S_t} \frac{n_i}{\sum_{i \in S_t} n_i} \Delta \mathbf{w}_i^{(t)}$$
(3)

B. Prior-Corrected Bayes Classifier

As introduced before, the *Label shift* induced non-IID data in FL refers to the label distribution changing between local training data and target test set. And we focus on the case where local training distributions have significant discrepancy to the uniform test distribution. We start by focusing on the calibration of a single classifier trained on one specific client. Let $P_s(X,Y)$ and $P_t(X,Y)$ denote the training (source) and the test (target) distributions, respectively. In a multi-class classification task, the final decision on the target distribution is often made by following the Bayes decision rule:

$$y^* = \arg\max_{y} P_t(y|x) = \arg\max_{y \in \mathcal{Y}} \frac{f_t(x|y)P_t(y)}{P_t(x)}$$
$$= \arg\max_{y \in \mathcal{Y}} f_t(x|y)P_t(y), \quad (4)$$

where $f_t(x|y)$ is the learned class conditional probability (likelihood) and $P_t(y)$ is the marginal label distribution (prior). Suppose that a discriminative model (e.g., softmax classifier) can perfectly learn the posterior distribution $P_s(Y|X)$ of the source dataset, then the corresponding Bayes classifier is defined as the following:

$$h_s(x) = \arg\max_{y \in \mathcal{V}} P_s(Y = y | X = x). \tag{5}$$

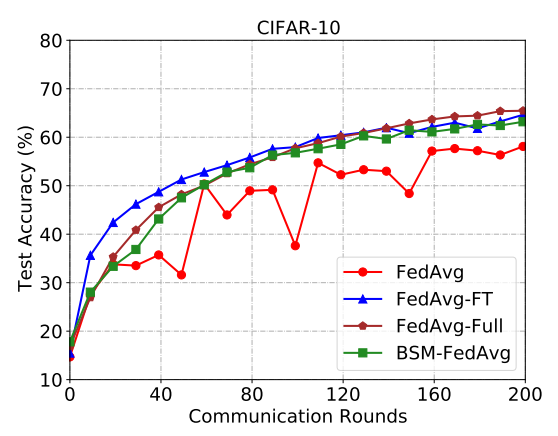


Fig. 1. Preliminary experimental results on CIFAR-10 dataset.

The classifier $h_s(x)$ is the optimal classifier on the training distribution. By further assuming that the test distribution has the same class conditional likelihood as the training set, i.e. $f_t(X|Y) = f_s(X|Y)$ and differs only on the class priors $P_t(Y) \neq P_s(Y)$. Then the optimal Bayes classifier on target distribution is given by the following expression:

$$h_t(x) = \arg\max_{y \in \mathcal{Y}} \frac{P_s(y|x)P_t(y)}{P_s(y)}.$$
 (6)

However, in the federated setting, samples on some labels might be totally missing for a local client, which would make the calibration ill-conditioned. One the other hand, notice that

$$h_t(x) = \arg\max_{y \in \mathcal{Y}} \frac{P_s(x, y)P_t(y)}{P_s(x)P_s(y)} = \arg\max_{y \in \mathcal{Y}} \frac{P_s(x|y)P_t(y)}{P_s(x)}. \quad (7)$$

Therefore, we can alternatively learn the class conditional likelihood $f_s(X|Y)$ on the training data by the technique of *Balanced-SoftMax*, which has been widely applied on long-tailed classification tasks [45], [46]. Specifically, for a data point (x_i, y_i) at client i, the log-loss is calculated by

$$\ell_i(x_j, y_j) = -\log\left(\frac{p_i(y_j)e^{z_j[y_j]}}{\sum_{c=1}^C p_i(c)e^{z_j[c]}}\right),\tag{8}$$

where $p_i(y)$ is the local prior of label y that can be estimated from the training data. Slightly different from the long-tailed classification, local prior probabilities of some classes could be zero in non-IID FL. Then, the inference on uniform distribution could be performed as the ordinary softmax classifier.

C. Preliminary Results

We conduct some preliminary experiments on CIFAR-10 to show that the unstable performance of FedAvg on non-IID data is mainly caused by the biased classifier head and the learned representation layers are still effective. To validate this, we assume that a small balanced set of samples is available at the server side for fine-tuning the classifier head in each round. We consider a setup with 50 clients, where each client has samples from only 2 classes and the successful transmission probability is 0.2 in each round. Three methods including vanilla FedAvg, FedAvg with balanced-softmax (BSM-FedAvg) and FedAvg with server-side fine-tuning (FedAvg-FT) are compared with

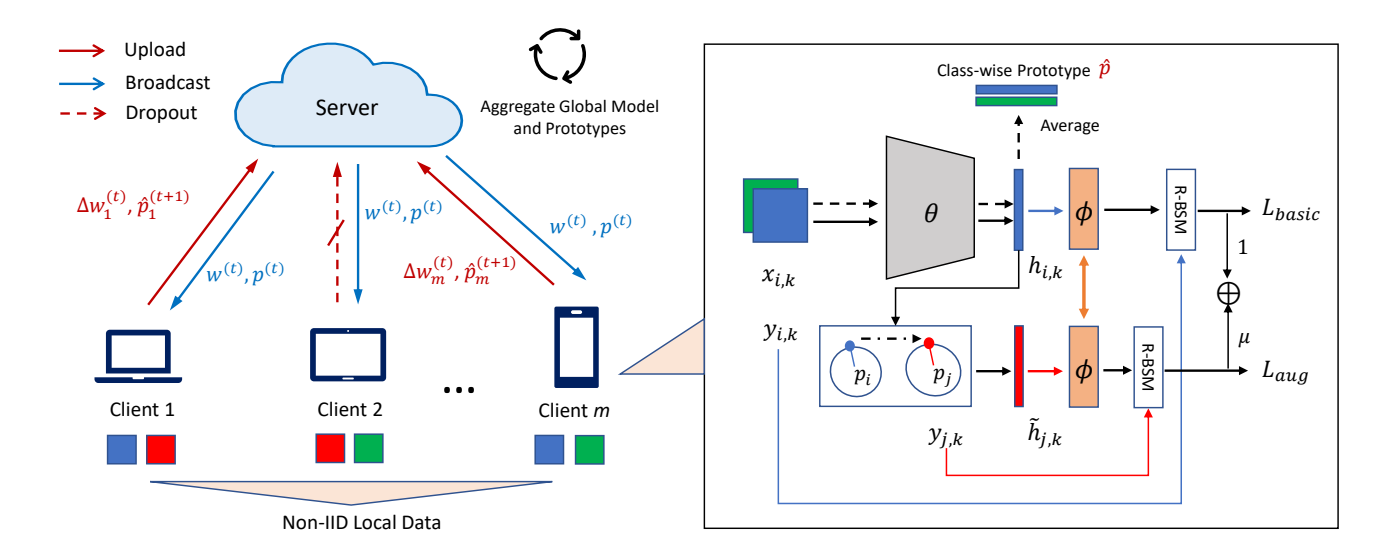


Fig. 2. Federated learning with a central server and a number of clients, where the clients may dropout during training. The local training consists of two key components, including relaxed balanced-softmax and feature-level augmentation by inter-class transfer.

learning curves plotted in Fig 1, where we also provide the result of FedAvg with full participation as a reference. The experimental results show that FedAvg with non-IID data and client dropout can result in severe performance fluctuating, while re-training the classifier on a small balanced set can significantly improve the stability and accuracy. On the other hand, it is interesting to see that BSM-FedAvg without the fine-tuning can almost approach the effect of head re-training. This preliminary results motivate us to learn a balanced classifier head without severe forgetting during the local training.

IV. OUR PROPOSED FRAMEWORK

In this section, we describe our framework for FL with non-IID data and client dropout as in Fig. 2 by introducing two bias-reduction methods in local training, including the modified cross-entropy computing and feature-level augmentation. It is worth noting that the central server is only responsible for message collection and aggregation without any extra model training or other complicated computation.

A. Relaxed Balanced-SoftMax Classifier

Although the balanced-softmax is effective in tackling the non-IID data to an extent, we claim that a combination of balanced-softmax and vanilla softmax could exhibit better performance in the case of pathological data setting where each client can only observe a few number of classes. As a conceptual example, consider an extreme case where each client only has samples from one class, then the balanced-softmax will result in zero loss and the local training will get stuck, while vanilla FedAvg could still update the model. Moreover, the classifier parameters corresponding to the missing classes could be too stale under the scheme of balanced-softmax, which might be sub-optimal for global aggregation and reduce the overall model performance. Therefore, we propose to use a linear combination of vanilla softmax and

balanced-softmax, which could be achieved by the following relaxed version of balanced-softmax (R-BSM):

$$\ell_i(x_j, y_j; \epsilon_i) = -\log\left(\frac{[\hat{p}_i(y_j)]e^{z_j[y_j]}}{\sum_{c=1}^C [\hat{p}_i(c)]e^{z_j[c]}}\right), \quad (9)$$

and the smoothed prior \hat{p}_i is obtained by

$$\hat{p}_i(y_j) = (1 - \epsilon_i) \cdot \frac{n_{i,j}}{n_i} + \epsilon_i \cdot \frac{1}{C},\tag{10}$$

where $\epsilon_i \in [0,1]$ is a positive and adjustable coefficient (usually small) added for client i. It is interesting to see that this form is very similar to the technique of label smoothing. However, employing label smoothing in local training of FL is not effective as we found in empirical evaluation.

To further analyze the effect of relaxed balanced-softmax, we represent the classifier parameters ϕ_i of the client i as the weight vectors $\{\phi_{i,c}\}_{c=1}^C$, where $\phi_{i,c}$ is named the c-th proxy as in [47]. For simplicity, we set all the bias vectors of the classifier as zeros and use the cross-entropy loss. Let $q_{j,c}$ denote the normalized score of class c for data point (\mathbf{x}_j, y_j) by the relaxed balanced-softmax, which is written by

$$q_{j,c} = \frac{\hat{p}_i(c)e^{\phi_{i,c}^{\mathsf{T}}\mathbf{h}_{y_j}}}{\sum_{c'=1}^{C}\hat{p}_i(c')e^{\phi_{i,c'}^{\mathsf{T}}\cdot\mathbf{h}_{y_j}}}$$
(11)

Then, the local objective function can be represented as:

$$\mathcal{L}_{i} = -\frac{1}{n_{i}} \sum_{j=1}^{n_{i}} \sum_{c=1}^{C} \mathbb{I}\left\{y_{j} = c\right\} \log\left(q_{j,c}\right), \tag{12}$$

where $\mathbf{h}_{i,y_j} = f_{\theta}(\mathbf{x}_j)$ is the feature embedding and θ denotes the feature extractor. The benefits of applying relaxed balanced-softmax are illustrated as follows.

Firstly, the smoothed prior can mitigate the staleness of proxies. For the c-th proxy $\phi_{i,c}$ of the i-th client, the positive features and negative features denote the features from the c-th class and other classes, respectively. The one-step update

of $\phi_{i,c}$ with the learning rate η can be computed as:

$$\Delta \phi_{i,c} = \underbrace{\frac{\eta}{n_i} \sum_{j=1, y_j=c}^{n_i} (1 - q_{j,c}) \mathbf{h}_j}_{\text{pulling by positive features}} - \underbrace{\frac{\eta}{n_i} \sum_{j=1, y_j \neq c}^{n_i} q_{j,c} \mathbf{h}_j}_{\text{pushing by negative features}}.$$
(13)

For class $c \in \{\mathcal{Y} \setminus \mathcal{Y}_i\}$, there is no update of $\phi_{i,c}$ under the original balanced-softmax scheme since the client does not hold any sample of class c and thus $p_i(c) = 0$. Therefore, not only there is no pulling force from positive features but also no pushing force from negative features exists due to $q_{j,c} \propto p_i(c)$. Under the scheme of vanilla softmax, the c-th proxy is only pushed away from negative features without any restriction from positive features and will result in inaccurate updating (catastrophic forgetting). By contrast, our relaxed version of balanced-softmax sets the prior of any missing class c a small value and thus restricts the pushing force from negative features, striking a balance between the staleness and inaccurate updating of the c-th proxy.

Secondly, the balanced classifier could mitigate inaccurate feature updating. Similarly, the update of \mathbf{h}_i is represented by:

$$\Delta \mathbf{h}_{j} = \underbrace{\frac{\eta}{n_{i}} \left(1 - q_{j,y_{j}} \right) \boldsymbol{\phi}_{i,y_{j}}}_{\text{pulling by positive proxy}} - \underbrace{\frac{\eta}{n_{i}}}_{\substack{c \in \mathcal{Y}_{i}, c \neq y_{j} \\ \text{pushing by negative proxies (II)}}}_{\substack{c \in \mathcal{Y} \setminus \mathcal{Y}_{i}, c \neq y_{j} \\ \text{pushing by negative proxies (II)}}}$$

$$(14)$$

Similar to the above analysis of proxy updates, the pushing force from any missing class c for updating feature embedding, i.e., the third term in Eq. (14), would disappear under both the vanilla softmax and balanced-softmax schemes, leading to inaccurate updates. Specifically, the balanced-softmax directly sets $q_{j,c}$ to zero while the vanilla softmax would result in significantly inaccurate proxy $\phi_{i,c}$ as local training going on and finally the $q_{j,c}$ would also be extremely small.

Finally, as the feature and classifier learning are highly coupled during the local training, mitigating the inaccurate updating of them can benefit each other and thus alleviate the performance degradation of federated learning with label skew.

B. Feature Augmentation for Missing Classes

Although the balanced-softmax can mitigate the impact of missing classes to an extent, the absence of training samples from those classes is still an issue remaining unsolved. One possible way is to generate synthetic data as augmented training samples. However, generating high-quality samples might be not practical in the resource constrained IoT scenarios as the training of generative model will involve high computation and communication costs. To remedy this, we propose to use a lightweight inter-class feature transfer approach to perform the feature augmentation for missing classes, aiming at training a classifier with better generalization ability.

Following the previous work in imbalanced learning [48], we assume that the feature $\mathbf{h}_{i,k}$ from *i*-th class lies in a Gaussian distribution with a class feature center \mathbf{p}_i , a.k.a, prototype,

and a covariance matrix Σ_i . The class-wise feature centers are estimated as an average over all feature vectors from the same class by a neural network as the feature extractor. To transfer the intra-class variance from local available classes to missing classes, we assume the covariance matrices are shared across all classes, i.e., $\Sigma_i = \Sigma$. Theoretically, the augmented feature sample for *i*-th class could be obtained by sampling a noise vector $\epsilon \sim \mathcal{N}(\mathbf{0}, \Sigma)$ and adding to its center \mathbf{p}_i . However, it is hard to accurately estimate the covariance matrix and the direction of noise vector might be too random. Therefore, we directly transfer the intra-class variance evaluated from the samples of available classes to the missing classes by linear translation and scaling. Specifically, our center-based feature transfer is achieved via:

$$\tilde{\mathbf{h}}_{ik} = \mathbf{p}_i + \lambda (\mathbf{h}_{ik} - \mathbf{p}_i), \tag{15}$$

where $\mathbf{h}_{i,k}$ and \mathbf{p}_i are the feature-level sample and the center of class i. \mathbf{p}_j is the feature center of a missing class j and $\tilde{\mathbf{h}}_{j,k}$ is the transferred feature for class j, preserving the same class identity as \mathbf{p}_j . This strategy is advantageous as it can be implemented efficiently without repeatedly computing the covariance matrix. The λ is an optional coefficient for scaling and we empirically find that set λ =1 by default is generally good. By sufficiently sampling $\mathbf{h}_{i,k}$ across different available classes, we expect to obtain an augmented distribution of missing class j in the feature space. A more efficient and effective implementation is augmenting all classes by enumerating the label set in a cyclic way until the mini-batch features are all utilized in each gradient decent step.

Algorithm 1 ReBaFL

Input: Learning rate η , communication rounds T, number of clients m, local epochs E, hyper-parameters ϵ and μ

Initialize: Initial model $w_0 \in R^d$

1: **for** t = 0, 1, ..., T - 1 **do**

Server Executes:

```
2: Broadcast \boldsymbol{w}^{(t)} and \boldsymbol{p}^{(t)} to clients
3: for each client i in active set S_t in parallel do
4: \Delta \boldsymbol{w}_i^{(t)}, \, \hat{\boldsymbol{p}}_i^{(t+1)} \leftarrow \mathbf{LocalTraining}(i, \, \boldsymbol{w}^{(t)}, \, \boldsymbol{p}^{(t)})
5: end for
6: Server aggregates \{\Delta \boldsymbol{w}_i^{(t)}\} and updates model:
7: \boldsymbol{w}^{(t+1)} = \boldsymbol{w}^{(t)} + \sum_{i \in S_t} \frac{n_i}{\sum_{i \in S_t} n_i} \Delta \boldsymbol{w}_i^{(t)}
8: Server aggregates prototypes, for c \in \mathcal{Y}:
9: \boldsymbol{p}^{(t+1)}[c] = \sum_{i \in S_t} \frac{n_{i,c}}{\sum_{i \in S_t} n_{i,c}} \hat{\boldsymbol{p}}_i^{(t+1)}[c]
10: end for
```

LocalTraining $(i, \boldsymbol{w}^{(t)}, \boldsymbol{p}^{(t)})$:

```
1: for local\ epoch\ e=0,1,...,E-1 do

2: for mini\ batch\ \xi_i\in\mathcal{D}_i do

3: Local update: \boldsymbol{w}_i^{(t)}\leftarrow\boldsymbol{w}_i^{(t)}-\eta\nabla_{\boldsymbol{w}}L_i(\boldsymbol{w}_i^{(t)})

4: end for

5: end for
```

6: Obtain local feature prototypes: $\hat{\pmb{p}}_i^{(t+1)}[c], \ c \in \mathcal{Y}_i$

7: **return**
$$\Delta oldsymbol{w}_i^{(t)} := oldsymbol{w}_i^{(t)} - oldsymbol{w}^{(t)}$$
 and $\hat{oldsymbol{p}}_i^{(t+1)}$ back

C. Algorithm Design

Local Optimization Objective. To strike a balance between exploring local knowledge and exploiting global knowledge, a client needs to update the local model by considering both local samples and global prototypes. To this end, we incorporate the designed relaxed softmax and feature-prototype based augmentation to learn a balanced classifier. The local objective function is defined as follows:

$$\min L_i(\boldsymbol{w}_i) := \frac{1}{|n_i|} \sum_{j=1}^{|n_i|} \left[\ell_i(\boldsymbol{w}_i; \xi_j) + \mu \cdot \ell_i(\boldsymbol{\phi}_i; \tilde{\mathbf{h}}_j) \right], \quad (16)$$

where $n_i = |\mathcal{D}_i|$ is the data size of client i, $\tilde{\mathbf{h}}_j$ is the augmented feature embedding based on the j-th data point and prototypes of class y_j and class $y_{j'} := [j \mod C]$, μ is a hyper-parameter to balance the two terms of loss. It is worth noting that the global prototypes might not contain all classes, therefore we only augment those available classes and re-calculate the prior of augmented features for computing the cross-entropy loss. Algorithm 1 summarizes the main workflow of ReBaFL, which implements the optimization steps in a client-server framework analogous to FedAvg.

Local Training Procedure. For local model training, the clients first replace the local model by the received global model:

$$\boldsymbol{w}_i^{(t)} \leftarrow \boldsymbol{w}^{(t)}. \tag{17}$$

Then, the class-wise prototypes are obtained by combining the received global prototypes $p^{(t)}$ and the newly computed local prototypes $p_i^{(t)}$ by the received feature extractor:

$$\boldsymbol{p}_{c}^{(t)} \leftarrow \boldsymbol{p}_{i}^{(t)}[c], \quad \forall c \in \mathcal{Y}_{i}.$$
 (18)

This step is designed mainly in consideration of the possible missing prototypes from previous round. Finally, the stochastic gradient decent (SGD) method will be applied to train the whole local model for multiple epochs:

$$\nabla_{\boldsymbol{w}} L_i(\boldsymbol{w}_i^{(t)}) = \nabla_{\boldsymbol{w}} \ell_i(\boldsymbol{w}_i^{(t)}; \xi_i) + \mu \nabla_{\boldsymbol{\phi}} \ell_i(\boldsymbol{\phi}_i^{(t)}; \mathbf{h}_i), \quad (19)$$

$$\boldsymbol{w}_{i}^{(t)} = \boldsymbol{w}_{i}^{(t)} - \eta \nabla_{\boldsymbol{w}} L_{i}(\boldsymbol{w}_{i}^{(t)}), \tag{20}$$

where the ξ_i denotes mini-batch data instead of a single data point in practical implementation. We also tried the decoupling strategy by alternatively training the representation layers and the classifier, which however presented little performance improvement and increased the local computation overhead as we found in numerical experiments. Therefore, we train the whole local model in an end-to-end manner as FedAvg, and the only changes we made include employing the relaxed balanced-softmax in computing the local cross-entropy loss and class-ordered cyclic feature-level augmentation.

Feature Statistics Extraction: After updating the local feature extractor, we compute the local feature centroid for each class through a single pass on the local dataset as follows,

$$\hat{\boldsymbol{p}}_{i,c}^{(t+1)} = \frac{\sum_{j=1}^{n_i} \mathbf{1}(y_j^{(i)} = c) \boldsymbol{f}_{\boldsymbol{\theta}_i^{(t+1)}}(x_j^{(i)})}{\sum_{j=1}^{n_i} \mathbf{1}(y_j^{(i)} = c)}, \quad \forall c \in \mathcal{Y}. \quad (21)$$

Global Model Aggregation Like the common algorithms, the server performs weighted averaging of local updated model parameters to obtain a new global model, with each coefficient determined by the local data size.

$$\mathbf{w}^{(t+1)} = \sum_{i=1}^{m} \alpha_i \mathbf{w}_i^{(t)}, \quad \alpha_i = \frac{n_i}{\sum_{i=1}^{m} n_i}.$$
 (22)

Update Global Feature Prototypes. After receiving the local feature prototypes, the following prototype aggregating operation is conducted to generate an estimated global prototype p_c for each class c.

$$\mathbf{p}_{c}^{(t+1)} = \frac{1}{\sum_{i=1}^{m} n_{i,c}} \sum_{i=1}^{m} n_{i,c} \hat{\mathbf{p}}_{i,c}^{(t+1)}, \quad \forall c \in \mathcal{Y}.$$
 (23)

When client dropout occurs, the server will not wait for all the m clients at each round but only collect messages from active clients within a pre-defined time to mitigate the impact of possible stragglers and improve the system efficiency.

D. Practical Consideration

Computation and Communication Costs. As mentioned before, our method does not change the main local training loop of FedAvg; we only compute local feature prototype for each class through one pass of local data, which induces negligible computation overhead. The transmission of class-wise feature prototypes will also only induce negligible communication overhead as the number of bits is much smaller than the size of exchanged parameters. Therefore, our proposed method could be implemented efficiently.

Privacy and Security Concerns. Generally, sharing the model parameters instead of the raw data can offer an extent of security guarantee, especially when local models are learned with large mini-batch size and multiple local training epochs. Our empirical verification will also confirm that the feature prototypes will not raise high privacy risks. Before performing aggregation in the server, anonymization mechanism such as random shuffling [49], [50] can also be applied to further enhance the privacy protection.

V. EVALUATION

In this section, we conduct various experiments to verify the effectiveness of our proposed method for improving model performance in the presence of non-IID data and client dropout. All experiments are implemented in PyTorch and simulated in NVIDIA GeForce RTX 3090 GPUs.

A. Experimental Setup

Datasets and Models. We conduct experiments of image classification tasks on two popular benchmark datasets, including Fashion-MNIST [51] and CIFAR-10 [52]. The Fashion-MNIST dataset contains 60,000 training samples and 10,000 testing samples from 10 categories of clothes. The CIFAR-10 dataset consists of 50,000 training samples and 10,000 testing samples, where the images contain more complex objects like cars, planes, and animals. We build a convolutional neural network (CNN) as the learning model for the Fashion-MNIST

dataset, which is constructed by two convolution layers with 16 and 32 channels respectively, each followed by a maxpooling layer, and two fully-connected (FC) layers with 128 and 10 units are used before softmax output. For the CIFAR-10 dataset, an extra convolution layer with 64 channels is added to enhance the model capacity.

Data Partitioning. Like previous studies [5], [11], we select a small set of samples from only a few classes as the local training data for each client. We assume each client i only has samples from N different classes. Specifically, we sample a subset $\mathcal{Y}_i \subseteq \mathcal{Y}$ with $|\mathcal{Y}_i| = N$, and randomly allocate n_i/N instances of each class in \mathcal{Y}_i to client i. In this paper, we set $n_i = 1000$ for all experiments. We focus on the pathological setting where each client only has samples from 2 classes, and also investigate another clustered setting where the clients are evenly divided into multiple groups and clients in the same group share a specific number of classes.

Compared Methods. We compare our method with the following commonly used baselines and start-of-the-art methods: vanilla FedAvg [5], FedProx [8], Scaffold [13], FedDyn [14], MOON [15], FedBABU [53] and FedRS [47], FedAvg with balanced-softmax (BSM-FedAvg) [54] and FedAvg with logit calibration (FedLC) [55]. For the baseline methods, we choose the recommended hyper-parameters as in the original papers. For our ReBaFL method, we tune ϵ over $\{0.001, 0.01, 0.1\}$ and μ over $\{0.1, 0.5, 1, 5\}$, and find that choosing $\epsilon = 0.01$ and $\mu = 0.1$ by default performs generally well for all experiments. Notice that we do not focus on tuning the best combination of hyper-parameters in our framework.

Training Settings. We consider a moderate-sized FL setup with m=20/50 clients and employ the mini-batch SGD as the local optimizer with batch size B=50 and weight decay 5e-4. The learning rate is set to 0.01 for Fashion-MNIST and 0.02 for CIFAR-10. For all experiments, the number of local training epochs between two consecutive communication rounds is selected as E=5. Each FL algorithm is trained for 200 communication rounds, which is enough for model convergence in our experiments.

Performance Metric. We evaluate the accuracy of global model on the balanced test set that has an uniform label distribution (10,000 test samples for each dataset), and report the average test accuracy for the last five rounds.

B. Main Results in Pathological Setting

Performance Comparison. We start from the random and independent straggler scenarios, which can be simulated by applying an unified successful transmission probability p for all clients. We evaluate all methods under the same conditions, presenting the test results in Table I. It can be found that our ReBaFL can consistently outperform other methods and achieve the highest average test accuracy for various cases. The results of FedAvg, FedProx and Scaffold also show that learning on non-IID data with client dropout is particularly difficult due to the unstable training induced by missing classes. Besides, it is worth noting that FedAvg is already a strong baseline, resulting in competitive or even better performance compared to various advanced algorithms.

TABLE I THE COMPARISON OF TEST ACCURACY (%) WITH SYSTEM SIZES M=20/50 and successful transmission probability p=0.5.

Method	Fashion-MNIST		CIFAR-10	
	$\overline{m=20}$	m = 50	$\overline{m=20}$	m = 50
FedAvg	75.27	83.60	54.82	64.37
FedProx	75.36	83.55	54.66	64.14
Scaffold	63.48	65.62	20.57	44.56
FedDyn	77.98	85.26	56.41	68.51
MOON	65.35	80.35	47.28	59.08
FedRS	72.46	79.83	54.39	64.05
FedBABU	74.20	82.34	52.73	62.19
FedLC	68.75	76.98	53.56	65.70
BSM-FedAvg	68.64	76.99	53.25	65.52
ReBaFL (ours)	78.81	85.44	58.49	68.59

Resilience to Client Dropout. To investigate the impact of client dropout, we also vary the p over $\{0.1, 0.3, 0.5\}$ in the setup of 50 clients. The results in Fig. 3 show that the high dropout rate would significantly degrade the performance of FedAvg and other methods that based on the vanilla softmax normalization during local training. Since the low participation rate cannot ensure that samples from all classes are available at each round, the global aggregation would not be able to correct the highly biased local classifier heads. In contrast, our method can stabilize the training performance and exhibit high robustness to various levels of client dropout. Besides, it can also be found that both FedRS and BSM-FedAvg that leverage the restricted softmax can already combat the label skew and client dropout with good training stability.

The above experimental results indicate that the conventional softmax-based training is vulnerable to the highly-skewed label distribution in FL and the high client dropout rate (i.e., low successful transmission probability) will further worsen the model performance. Instead, applying the balanced-softmax mechanism is usually beneficial and robust to label distribution skew. And our proposed relaxed version of balanced-softmax equipped with feature augmentation can overcome such label skew and client dropout to a larger extent and achieve better model performance.

C. Main Results in Clustered Setting

In this setting, we assume that the clients have clustered structures and consider a setup with 20 clients which are grouped into 5 clusters. In each cluster, the clients share the same number of available classes and the same successful transmission probability, while those quantities could vary across different clusters. In such cases, it is of significant importance to ensure the stability of FL training. We set the number of class N by $\{2,2,3,3,5\}$ and the p by $\{0.5,0.5,0.3,0.3,0.2\}$ for each cluster, respectively. Notice that even the clients within the same cluster may have substantially distinct subsets of labels. The main results are presented in Fig. 4 and Fig. 5, from which we can see that, overall, the

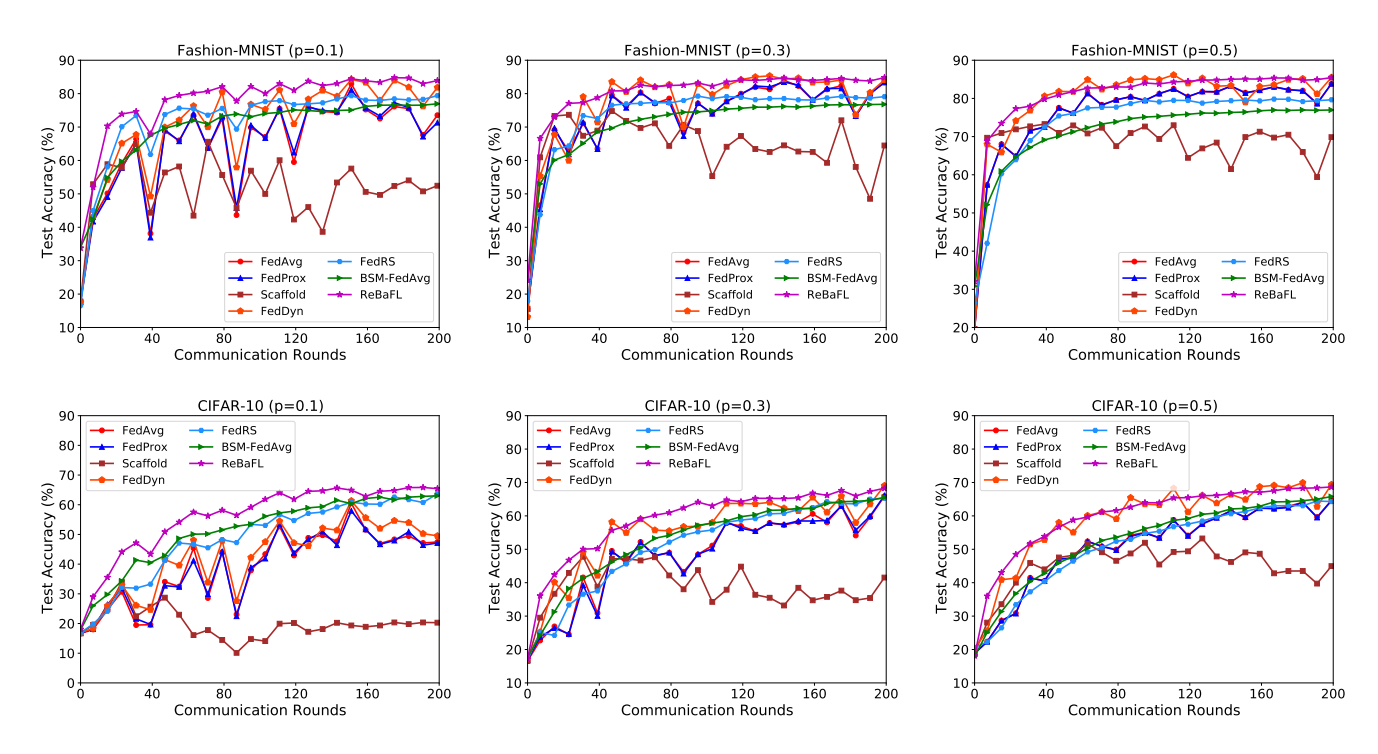


Fig. 3. Test accuracy over communication rounds under different levels of client dropout. Each client only has two randomly allocated labels.

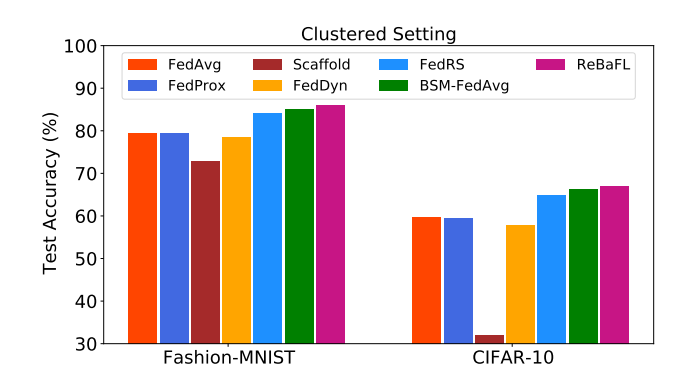


Fig. 4. Performance comparison in clustered setting. Objective calibration-based methods outperform regularization-based methods with large margins.

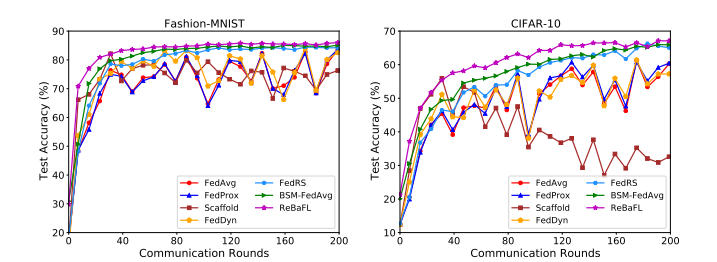


Fig. 5. Test accuracy over communication rounds in clustered setting. ReBaFL can present fast convergence and better model accuracy.

ReBaFL still achieves the best model performance and training stability during the federation procedure with client dropout. In this setting, the FedDyn tends to be as unstable as FedAvg due to label distribution skewness and unexpected client dropout. It can also be found that BSM-FedAvg and FedRS also present good performance since the data heterogeneity is relatively

mild compared to the pathological setting.

D. Ablation Studies

1) Effects of Designed Components: We have two key designed components in ReBaFL, i.e., relaxed balanced-softmax (R-BSM) and feature augmentation (F-Aug). Here we conduct ablation studies to verify the individual efficacy of those two components. We test the CIFAR-10 dataset under both Pathological and Clustered settings, reporting the resulted model accuracy. As demonstrated in Table II, the relaxed-softmax alonecan already provide a significant improvement of the model accuracy and the combination of those two components is able to achieve the most satisfactory performance and exceed the baseline with a large margin. One thing interesting we can see is that the inter-class feature transfer based augmentation can even worsen the model performance when the balanced softmax is not applied.

TABLE II
MODEL ACCURACY (%) WITH DIFFERENT DESIGN COMPONENTS

R-BSM	F-Aug	Data Settings		
K-DSM		Pathological	Clustered	
		54.82	59.71	
\checkmark		56.71	65.75	
	\checkmark	54.01	58.85	
√	✓	58.49	67.12	

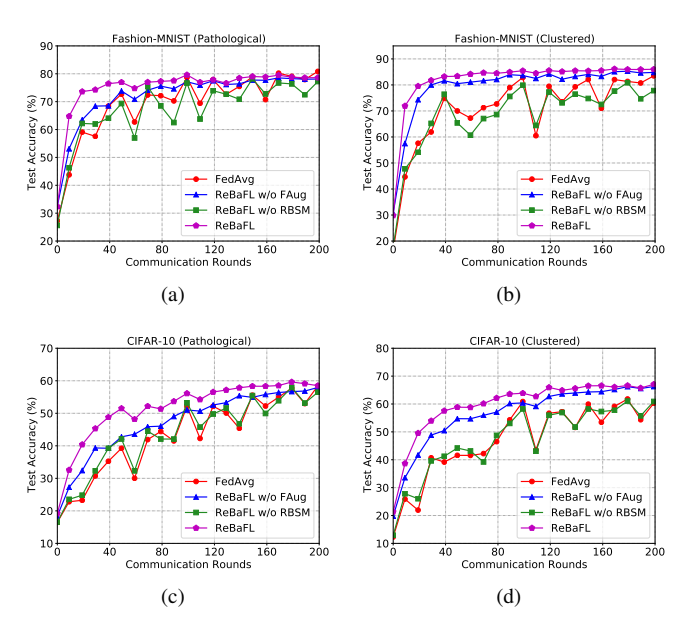


Fig. 6. Learning curves for ablation studies. (a)(c) are in pathological setting on two datasets while (b)(d) are in clustered setting.

2) Diversity of Local Models: We also record the model weight diversity among collected clients across the training process, where the weight diversity is defined as follows.

$$\Lambda^{(t)} := \frac{1}{|S_t|} \sum_{i \in S_t} \| \boldsymbol{w}_i^{(t)} - \bar{\boldsymbol{w}}^{(t)} \|_2^2, \tag{24}$$

where $\bar{w}^{(t)}$ is the average of local models. The results in Fig. 7 indicate that our proposed balanced softmax can effectively reduce the weight diversity and thus facilitate the model aggregation, resulting in a better global model. Interestingly, we can find that when the feature augmentation is applied, the weight diversity will slightly increase as different clients may have various kinds of training samples and the calibration of local classifier also has some non-zero diversity across clients. However, the empirical results in the main evaluation clearly shows that the feature augmentation could benefit the federated learning by accelerating the model convergence and improving the final model accuracy. Possible explanation towards this phenomenon might be that slight noise in stochastic gradients can enhance the generalization of the trained model [56].

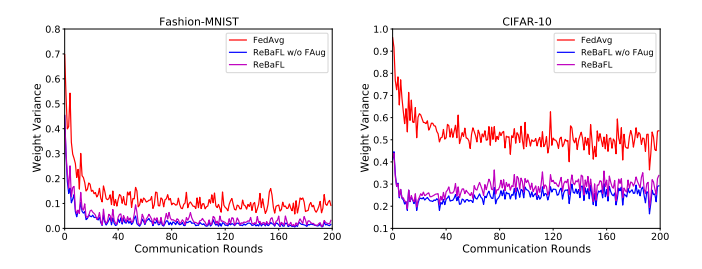


Fig. 7. Local model parameter diversity over training rounds.

E. Further Discussions

Finally, we perform some analyses and discussions on some factors that may affect the performance of our method. Specifically, we evaluate our method with different choices of hyper-parameters, local training epochs, straggling behavior transition periods, and system sizes.

1) Impact of Hyper-parameters: There are mainly two hyper-parameters (ϵ and μ) in our framework, however, simultaneously tuning them is still time-consuming. Here we choose to incrementally add those two components by first investigating the ϵ to find a suitable value, then and tuning the μ with the selected ϵ^* fixed. Specifically, we vary the value of ϵ over $\{1e - 4, 1e - 3, 1e - 2, 1e - 1, 2e - 1\}$ with $\mu * = 0$ and vary the value of μ over $\{0, 0.1, 0.5, 1.0, 5.0\}$ with $\epsilon^* = 0.01$. The results are presented in Fig. 8, from which we can find that a relative large ϵ will cause the training unstable but a too small value will reduce the model performance, indicating the importance of a suitable value of ϵ . Similarly, a proper selection of μ is also needed. However, the best values of hyper-parameters may vary among specific learning tasks. As mentioned before, we do not aim at finding the best combination of hyper-parameters and the empirical studies demonstrate that relatively small values are preferred.

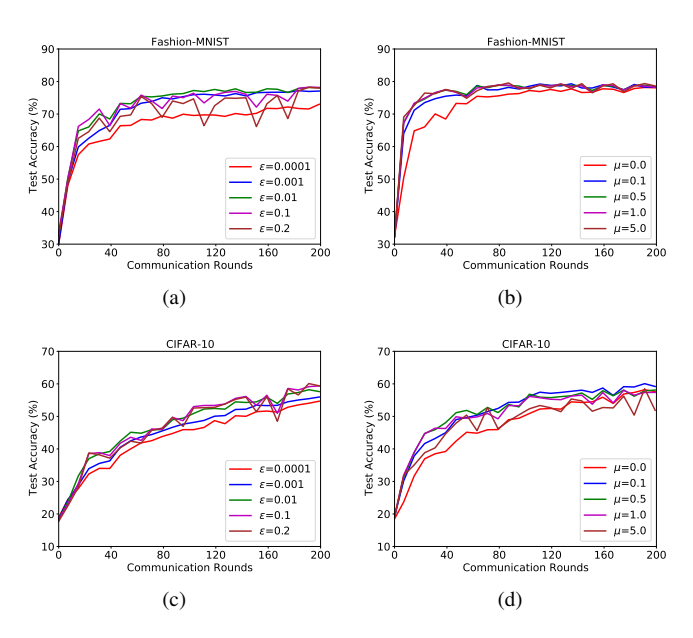


Fig. 8. Performance comparison with varying hyper-parameters.

2) Impact of Local Epochs: In this part, we add more computation per client on each round by increasing the local epochs E. To reduce communication overhead, the clients tend to have more local training steps, which can lead to less global communication and thus faster convergence. Therefore, we conduct many experiments on CIFAR-10 dataset with 20 clients by varying the epochs over $\{1, 2, 5, 10, 20\}$. As shown in Tab. 9, our method is superior to other baselines by a large margin. Given limited communication rounds, the model is not well trained for all methods when the number of local updates is too small. For a large value of E, while the performance gap of these baselines is relatively small, our approach still consistently outperforms other methods. The results also show that larger values of E will only slightly hurt the model accuracy under our framework, while FedAvg results in more obvious accuracy degradation. Nevertheless, there is a trade-

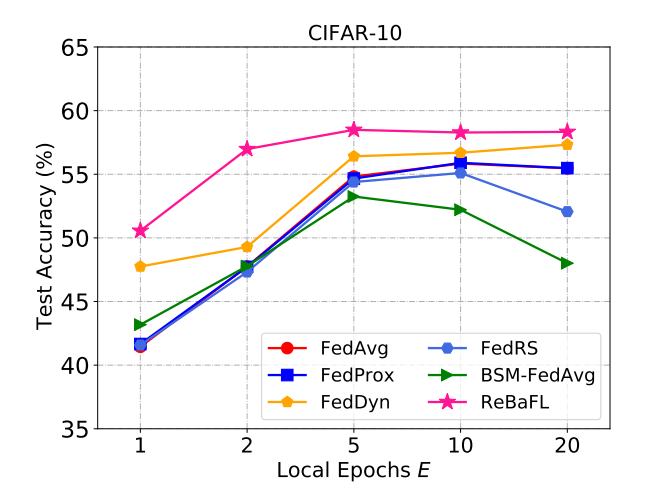


Fig. 9. Performance comparison on CIFAR-10 dataset with varying local epochs. The number of communication rounds is fixed.

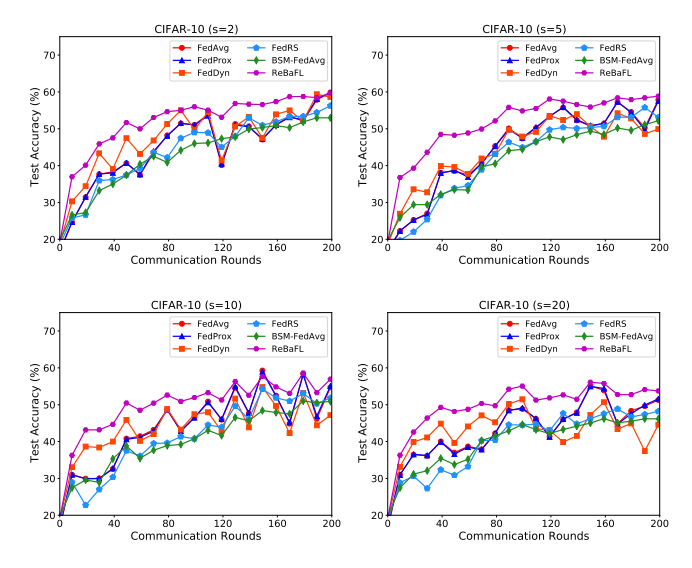


Fig. 10. Performance comparison on CIFAR-10 dataset with varying straggling periods. The active status of each client is changed with probability p at a interval of s rounds.

off between the computations and communications, i.e., larger E requires more computations at local clients, while smaller E needs more global communication rounds to converge.

3) Impact of Straggling Behaviors: In the above experiments, we always assume that the client dropout is occurred with a given probability and is independent across communication rounds, which however could only cover a limited scenario as a straggling or inactive client might persist for a long period so as for a active client. Therefore, we investigate the impact of persistent straggling behaviors by adjusting the active states with a varying period $s \in \{2, 5, 10, 20\}$, where we conduct a random selection of dropout clients at intervals of every s rounds. From the curves in Fig. 10, it can be found that the straggling period has a non-negligible impact on the federated learning as in each period some classes may be missing among the active clients and the learned global model is biased such that the test accuracy might decrease in a extent. Nevertheless, our method still exhibits

the best performance across different straggling behaviors, demonstrating its robustness and stability against the client dropout in cross-device FL scenarios.

4) System Scalability: To further verify the adaptability and scalability of our method, we compare the results of three different large system sizes, where we set 100, 200 and 500 clients with different local data sizes to ensure disjoint data allocation. We allocate 2 classes and k samples per class for each client, where we adjust the k under different system sizes by keeping km = 50,000. Here we simply select 10% clients in each communication round at random for each setup. We compare our method with the baselines and report the results in Table III. As expected, our method consistently outperforms other baselines across all settings, validating its adaptability and robustness in a variety of federated environments. It can be seen that the performance of all methods decreases with mincreasing. We conjecture that the reason is that more clients will make the local models more diverse and hurt the global aggregation. However, our method can still achieve 46.67% accuracy when there are 500 clients.

TABLE III

THE TEST ACCURACY (%) WITH VARYING NUMBER OF CLIENTS (m) ON CIFAR-10. CLIENT SAMPLING RATE IS 0.1 FOR ALL SETTINGS.

Method	System Size				
	m = 100	m = 200	m = 500		
FedAvg	55.78	47.53	33.78		
FedProx	56.81	47.49	33.81		
Scaffold	63.36	47.66	16.12		
FedDyn	63.35	53.58	37.74		
MOON	50.53	42.47	26.89		
FedRS	60.85	51.86	42.12		
FedBABU	52.65	43.62	33.41		
BSM-FedAvg	60.32	51.75	43.36		
ReBaFL (ours)	63.89	57.23	46.67		

F. Testing Data Leakage from Prototypes

Finally, we study the potential privacy leakage risk during the training of ReBaFL. Since our training process is involved with the sharing of feature prototypes for each class, we consider the honest-but-curious setting where both server and clients follow the system protocol exactly as specified, but may try to infer other parties' private information based on the received feature prototypes. We simulate the scenarios with possible information leakage risks by presenting several data leakage attacks on CIFAR-10 dataset, including upconvolutional neural network (UpCNN) [57] and variational autoencoder (VAE) [58] that try to recover the input images from the feature representations. And we also adopt the approach from the state-of-the-art gradient attack generative regression neural network (GRNN) [59] to inverse the feature prototypes. From the reconstructed results in Fig. 11, we can conclude that sharing feature prototypes will neither leak considerable information about the raw data, nor will they reveal any relationship between different image categories.

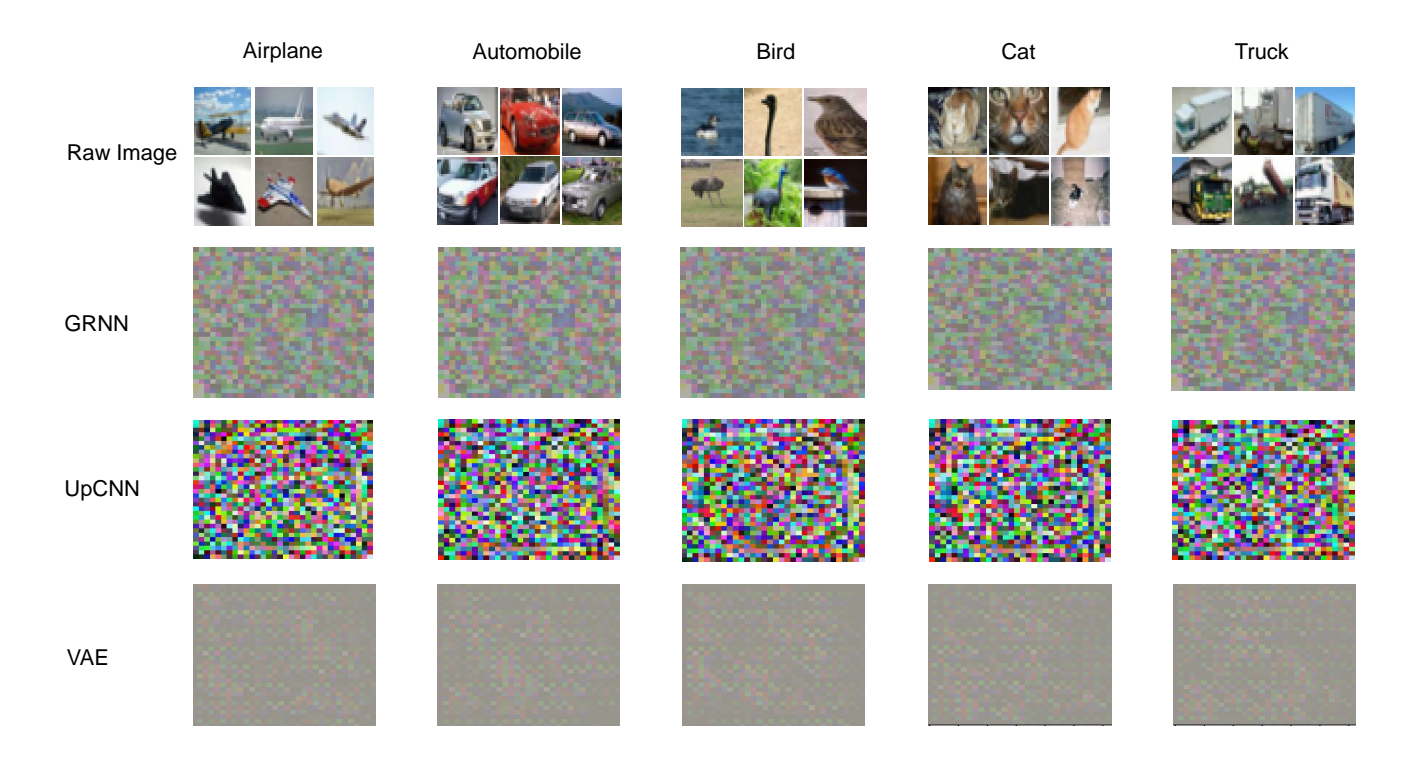


Fig. 11. Reconstruction results of various invert attacks on the feature prototypes. No semantically meaningful information can be extracted by the attacks.

The reasons why feature prototypes are difficult to invert may be in three-fold. First, the private information contained by the low-dimensional feature representation is much less than the high-dimensional gradient, thus even the successful gradient attack might fail to infer raw data from feature prototypes. Second, the feature prototype is an average of per-image feature vectors and the characteristics of individual images could be concealed. Third, the numerous non-linear transformations in the hidden layers of complex neural networks make it hard to invert images by only aligning the feature representations. This is also consistent with the phenomenon that reconstruction from the shallow representations is easier than from the representations generated by the deep fully-connected layers [57].

VI. CONCLUSION

In this paper, we introduce the relaxed balanced-softmax and the cross-class transfer-based feature augmentation for stabilizing and enhancing the federated learning with non-IID data and client dropout. Extensive empirical evaluations are provided to verify the effectiveness and robustness of our framework in a wide variety of settings. We also evaluate image invert attacks on the feature prototypes to demonstrate that the sharing of prototypes will not induce high privacy leakage risks. Future work may include investigating the application of our algorithm in more complex settings, e.g., decentralized systems or clients with dynamic data distributions. More effective methods of global model aggregation for heterogeneous FL also need further exploration.

REFERENCES

- [1] G. Hinton, L. Deng, D. Yu, G. E. Dahl, A. Mohamed, N. Jaitly, A. Senior, V. Vanhoucke, P. Nguyen, T. N. Sainath, and B. Kingsbury, "Deep neural networks for acoustic modeling in speech recognition," *IEEE Signal Processing Magazine*, vol. 29, no. 6, pp. 82–97, 2012.
- [2] V. Hayyolalam, M. Aloqaily, Ö. Özkasap, and M. Guizani, "Edge-assisted solutions for iot-based connected healthcare systems: A literature review," *IEEE Internet Things J.*, vol. 9, no. 12, pp. 9419–9443, 2022.
- [3] Z. Ullah, F. Al-Turjman, L. Mostarda, and R. Gagliardi, "Applications of artificial intelligence and machine learning in smart cities," *Comput. Commun.*, vol. 154, pp. 313–323, 2020.
- [4] S. Sharma, Data privacy and GDPR handbook. John Wiley & Sons, 2019.
- [5] B. McMahan, E. Moore, D. Ramage, S. Hampson, and B. A. y Arcas, "Communication-efficient learning of deep networks from decentralized data," in *International Conference on Artificial Intelligence and Statis*tics, AISTATS, 2017.
- [6] Q. Yang, Y. Liu, T. Chen, and Y. Tong, "Federated machine learning: Concept and applications," ACM Trans. Intell. Syst. Technol., vol. 10, no. 2, Jan. 2019.
- [7] T. Li, A. K. Sahu, A. Talwalkar, and V. Smith, "Federated learning: Challenges, methods, and future directions," *IEEE Signal Process. Mag.*, vol. 37, no. 3, pp. 50–60, 2020.
- [8] T. Li, A. K. Sahu, M. Zaheer, M. Sanjabi, A. Talwalkar, and V. Smith, "Federated optimization in heterogeneous networks," in *Proceedings of Machine Learning and Systems* 2020, MLSys, 2020.
- [9] O. A. Wahab, A. Mourad, H. Otrok, and T. Taleb, "Federated machine learning: Survey, multi-level classification, desirable criteria and future directions in communication and networking systems," *IEEE Commun. Surv. Tutorials*, vol. 23, no. 2, pp. 1342–1397, 2021.
- [10] P. Kairouz, H. B. McMahan, B. Avent, A. Bellet, M. Bennis, and et al, "Advances and open problems in federated learning," *Found. Trends Mach. Learn.*, vol. 14, no. 1-2, pp. 1–210, 2021.
- [11] Y. Zhao, M. Li, L. Lai, N. Suda, D. Civin, and V. Chandra, "Federated learning with non-iid data," arXiv:1806.00582, 2018.
- [12] S. Wang, T. Tuor, T. Salonidis, K. K. Leung, C. Makaya, T. He, and K. Chan, "Adaptive federated learning in resource constrained edge computing systems," *IEEE J. Sel. Areas Commun.*, vol. 37, no. 6, pp. 1205–1221, 2019.

- [13] S. P. Karimireddy, S. Kale, M. Mohri, S. J. Reddi, S. U. Stich, and A. T. Suresh, "SCAFFOLD: stochastic controlled averaging for federated learning," in *Proceedings of the 37th International Conference* on Machine Learning, ICML, 2020.
- [14] D. A. E. Acar, Y. Zhao, R. M. Navarro, M. Mattina, P. N. Whatmough, and V. Saligrama, "Federated learning based on dynamic regularization," in 9th International Conference on Learning Representations, ICLR, 2021.
- [15] Q. Li, B. He, and D. Song, "Model-contrastive federated learning," in IEEE Conference on Computer Vision and Pattern Recognition, CVPR, 2021.
- [16] Q. Li, Y. Diao, Q. Chen, and B. He, "Federated learning on non-iid data silos: An experimental study," *CoRR*, vol. abs/2102.02079, 2021. [Online]. Available: https://arxiv.org/abs/2102.02079
- [17] M. Luo, F. Chen, D. Hu, Y. Zhang, J. Liang, and J. Feng, "No fear of heterogeneity: Classifier calibration for federated learning with non-iid data," *CoRR*, vol. abs/2106.05001, 2021. [Online]. Available: https://arxiv.org/abs/2106.05001
- [18] E. Ozfatura, K. Ozfatura, and D. Gündüz, "Fedadc: Accelerated federated learning with drift control," in *IEEE International Symposium on Information Theory*, ISIT, 2021.
- [19] T. H. Hsu, H. Qi, and M. Brown, "Federated visual classification with real-world data distribution," in *Computer Vision - ECCV 2020 - 16th European Conference*, 2020.
- [20] L. Wang, S. Xu, X. Wang, and Q. Zhu, "Addressing class imbalance in federated learning," in *Thirty-Fifth AAAI Conference on Artificial Intelligence*, AAAI, 2021.
- [21] T. Yoon, S. Shin, S. J. Hwang, and E. Yang, "Fedmix: Approximation of mixup under mean augmented federated learning," in 9th International Conference on Learning Representations, ICLR, 2021.
- [22] H. Wang, Z. Kaplan, D. Niu, and B. Li, "Optimizing federated learning on non-iid data with reinforcement learning," in *IEEE Conference on Computer Communications, INFOCOM*, 2020.
- [23] M. Tang, X. Ning, Y. Wang, Y. Wang, and Y. Chen, "Fedgp: Correlation-based active client selection for heterogeneous federated learning," *CoRR*, vol. abs/2103.13822, 2021. [Online]. Available: https://arxiv.org/abs/2103.13822
- [24] Y. Fraboni, R. Vidal, L. Kameni, and M. Lorenzi, "Clustered sampling: Low-variance and improved representativity for clients selection in federated learning," in *Proceedings of the 38th International Conference* on Machine Learning, ICML, 2021.
- [25] H. Chen and W. Chao, "Fedbe: Making bayesian model ensemble applicable to federated learning," in *International Conference on Learning Representations*, ICLR, 2021.
- [26] T. Lin, L. Kong, S. U. Stich, and M. Jaggi, "Ensemble distillation for robust model fusion in federated learning," in Advances in Neural Information Processing Systems 33: Annual Conference on Neural Information Processing Systems, NeurIPS, 2020.
- [27] Z. Zhu, J. Hong, and J. Zhou, "Data-free knowledge distillation for heterogeneous federated learning," in *Proceedings of the 38th International* Conference on Machine Learning, ICML, 2021.
- [28] V. Kulkarni, M. Kulkarni, and A. Pant, "Survey of personalization techniques for federated learning," in Fourth World Conference on Smart Trends in Systems, Security and Sustainability (WorldS4), 2020.
- [29] C. T. Dinh, N. H. Tran, and T. D. Nguyen, "Personalized federated learning with moreau envelopes," in *Conference on Neural Information Processing Systems, NeurIPS*, 2020.
- [30] A. Fallah, A. Mokhtari, and A. E. Ozdaglar, "Personalized federated learning with theoretical guarantees: A model-agnostic meta-learning approach," in Advances in Neural Information Processing Systems, NeurIPS, 2020.
- [31] L. Collins, H. Hassani, A. Mokhtari, and S. Shakkottai, "Exploiting shared representations for personalized federated learning," in *Proceedings of the 38th International Conference on Machine Learning, ICML*, 2021.
- [32] A. Ghosh, J. Chung, D. Yin, and K. Ramchandran, "An efficient framework for clustered federated learning," arXiv preprint arXiv:2006.04088, 2020
- [33] Y. Mansour, M. Mohri, J. Ro, and A. T. Suresh, "Three approaches for personalization with applications to federated learning," arXiv preprint arXiv:2002.10619, 2020.
- [34] F. Sattler, K. Müller, and W. Samek, "Clustered federated learning: Model-agnostic distributed multitask optimization under privacy constraints," *IEEE Trans. Neural Networks Learn. Syst.*, vol. 32, no. 8, pp. 3710–3722, 2021.

- [35] Y. Chen, Y. Ning, M. Slawski, and H. Rangwala, "Asynchronous online federated learning for edge devices with non-iid data," in *IEEE International Conference on Big Data* (BigData), 2020.
- [36] W. Wu, L. He, W. Lin, R. Mao, C. Maple, and S. A. Jarvis, "SAFA: A semi-asynchronous protocol for fast federated learning with low overhead," *IEEE Trans. Computers*, vol. 70, no. 5, pp. 655–668, 2021.
- [37] X. Gu, K. Huang, J. Zhang, and L. Huang, "Fast federated learning in the presence of arbitrary device unavailability," in *Annual Conference* on Neural Information Processing Systems, NeurIPS, 2021.
- [38] L. Zhu, H. Lin, Y. Lu, Y. Lin, and S. Han, "Delayed gradient averaging: Tolerate the communication latency for federated learning," in Advances in Neural Information Processing Systems 34: Annual Conference on Neural Information Processing Systems, NeurIPS, 2021.
- [39] A. Reisizadeh, I. Tziotis, H. Hassani, A. Mokhtari, and R. Pedarsani, "Straggler-resilient federated learning: Leveraging the interplay between statistical accuracy and system heterogeneity," *IEEE J. Sel. Areas Inf. Theory*, vol. 3, no. 2, pp. 197–205, 2022.
- [40] B. Luo, W. Xiao, S. Wang, J. Huang, and L. Tassiulas, "Tackling system and statistical heterogeneity for federated learning with adaptive client sampling," in *IEEE INFOCOM 2022 - IEEE Conference on Computer Communications*, 2022.
- [41] Z. Ma, Y. Xu, H. Xu, Z. Meng, L. Huang, and Y. Xue, "Adaptive batch size for federated learning in resource-constrained edge computing," *IEEE Transactions on Mobile Computing*, pp. 1–1, 2021.
- [42] L. Li, M. Duan, D. Liu, Y. Zhang, A. Ren, X. Chen, Y. Tan, and C. Wang, "Fedsae: A novel self-adaptive federated learning framework in heterogeneous systems," in *International Joint Conference on Neural Networks, IJCNN*, 2021.
- [43] D. Jhunjhunwala, P. Sharma, A. Nagarkatti, and G. Joshi, "Fedvarp: Tackling the variance due to partial client participation in federated learning," in *Proceedings of the Thirty-Eighth Conference on Uncer*tainty in Artificial Intelligence, UAI, 2022.
- [44] H. Wang and J. Xu, "Friends to help: Saving federated learning from client dropout," *CoRR*, vol. abs/2205.13222, 2022. [Online]. Available: https://doi.org/10.48550/arXiv.2205.13222
- [45] J. Ren, C. Yu, S. Sheng, X. Ma, H. Zhao, S. Yi, and H. Li, "Balanced meta-softmax for long-tailed visual recognition," in *Annual Conference* on Neural Information Processing Systems, NeurIPS, 2020.
- [46] J. Tian, Y. Liu, N. Glaser, Y. Hsu, and Z. Kira, "Posterior re-calibration for imbalanced datasets," in *Annual Conference on Neural Information Processing System, NeurIPS*, 2020.
- [47] X. Li and D. Zhan, "Feders: Federated learning with restricted softmax for label distribution non-iid data," in KDD '21: The 27th ACM SIGKDD Conference on Knowledge Discovery and Data Mining. ACM, 2021.
- [48] X. Yin, X. Yu, K. Sohn, X. Liu, and M. Chandraker, "Feature transfer learning for face recognition with under-represented data," in *IEEE Conference on Computer Vision and Pattern Recognition, CVPR*, 2019.
- [49] R. Liu, Y. Cao, H. Chen, R. Guo, and M. Yoshikawa, "FLAME: differentially private federated learning in the shuffle model," in *Thirty-Fifth AAAI Conference on Artificial Intelligence*, AAAI, 2021.
- [50] A. M. Girgis, D. Data, S. N. Diggavi, P. Kairouz, and A. T. Suresh, "Shuffled model of differential privacy in federated learning," in *The* 24th International Conference on Artificial Intelligence and Statistics, AISTATS, 2021.
- [51] H. Xiao, K. Rasul, and R. Vollgraf, "Fashion-mnist: a novel image dataset for benchmarking machine learning algorithms," *CoRR*, vol. abs/1708.07747, 2017.
- [52] A. Krizhevsky and G. Hinton, "Learning multiple layers of features from tiny images," *University of Toronto*, 2009.
- [53] J. Oh, S. Kim, and S. Yun, "Fedbabu: Toward enhanced representation for federated image classification," in *The Tenth International Confer*ence on Learning Representations, ICLR, 2022.
- [54] H. Chen and W. Chao, "On bridging generic and personalized federated learning for image classification," in *The Tenth International Conference* on Learning Representations, ICLR, 2022.
- [55] J. Zhang, Z. Li, B. Li, J. Xu, S. Wu, S. Ding, and C. Wu, "Federated learning with label distribution skew via logits calibration," in *Interna*tional Conference on Machine Learning, ICML, 2022.
- [56] S. L. Smith, E. Elsen, and S. De, "On the generalization benefit of noise in stochastic gradient descent," in *Proceedings of the 37th International Conference on Machine Learning, ICML*, 2020.
- [57] A. Dosovitskiy and T. Brox, "Inverting visual representations with convolutional networks," in *IEEE Conference on Computer Vision and Pattern Recognition, CVPR*, 2016.
- [58] D. P. Kingma and M. Welling, "Auto-encoding variational bayes," in 2nd International Conference on Learning Representations, ICLR, 2014.

[59] H. Ren, J. Deng, and X. Xie, "GRNN: generative regression neural network - A data leakage attack for federated learning," *ACM Trans. Intell. Syst. Technol.*, vol. 13, no. 4, pp. 65:1–65:24, 2022.